Heliyon 6 (2020) e04392

Contents lists available at ScienceDirect

Heliyon

journal homepage: www.cell.com/heliyon

Research article

Alpha glucosidase inhibition activity of phenolic fraction from *Simarouba glauca*: An *in-vitro*, *in-silico* and kinetic study

Kirana P. Mugaranja [a,b], Ananda Kulal [a,*]

[a] *Biological Sciences Division, Poornaprajna Institute of Scientific Research, Bidalur Post, Devanahalli, Bangalore Rural, 562110, India*
[b] *Manipal Academy of Higher Education, Manipal, 576104, India*

ARTICLE INFO

Keywords:
Food science
Food chemistry
Agriculture
Alpha glucosidas
Enzyme kinetics
Anti-diabetic
Molecular docking
Medicinal plant
Hypoglycaemic

ABSTRACT

A phenolic rich fraction purified from *Simarouba glauca* leaves was effective in alpha glucosidase inhibition. The purified fraction named 'fraction-14' had shown significant inhibition of yeast alpha glucosidase enzyme activity ($IC_{50} = 2.4 \pm 0.4$ μg/mL) when compared to anti-diabetic drug acarbose ($IC_{50} = 2450 \pm 24$ μg/mL). The purified fraction also had reasonable DPPH ($IC_{50} = 14.4 \pm 0.1$ μg/mL) and ABTS ($IC_{50} = 7.6 \pm 0.5$ μg/mL) free radical scavenging activity when compared to the standard ascorbic acid. The LC-MS analysis of bioactive 'fraction-14' revealed four compounds, eclalbasaponin-v (**1**), cyanidin-3-O-(2′galloyl)-galactoside (**2**), kaempferol-3-O-glucoside (**3**) and kaempferol-3-O-pentoside (**4**) for the first time in *S. glauca* in this study. The kinetic study of the 'fraction-14' indicates a mixed type of inhibition on the alpha glucosidase enzyme with K_i, 6.2 μg/mL. Docking studies showed promising binding energy for the compounds **2** (-7.769 kJ/mol), **3** (-7.04 kJ/mol) and **4** (-7.127 kJ/mol) against yeast alpha glucosidase which was better than acarbose (-6.867 kJ/mol). In conclusion, the phenolic rich fraction from *S. glauca* possessing good *in-vitro* antioxidant property and alpha glucosidase enzyme inhibition potential along with mixed inhibition kinetics. Also, better binding energy of compounds (**1, 2 & 3**) appears to contain potential lead-molecule for antidiabetic therapy.

1. Introduction

Diabetes Mellitus (DM) is known as one of the largest global threats of the 21st century in developed countries as well as in developing countries. Type 2 diabetes mellitus (T2DM) is characterized by constant hyperglycaemia due to the condition called insulin resistance in targeted organs and pancreatic β cell dysfunction, leading to deterioration in insulin secretions (Chatterjee et al., 2017). A survey from the International Diabetes Federation (IDF) in 2017 stated that globally 425 million people are suffering from DM in which more than 90 % of them have T2DM and, 629 million people may get diabetes by 2045 (Cho et al., 2018). Factors such as genetic susceptibility, environmental factors, obesity, physical inactivity, high sugar, fat-rich diets, etc. are believed to be responsible for the pathogenesis of T2DM. For the treatment of T2DM, several oral medications as well as injectable drugs have been available for decades, targeting a different kind of organ systems. Nevertheless, the main strategies of T2DM drugs are directed towards the control of hyperglycaemia and maintenance of the normal blood glucose homeostasis in the body (Kahn et al., 2014).

Amongst the many drug targets of T2DM, starch digesting enzymes such as alpha amylase and intestinal alpha glucosidase are targeted to achieve inhibition of these enzymes and hence to control the post-prandial hyperglycaemia. Alpha glucosidases [EC 3.2.1.20] are digestive enzymes that belong to a family called 'glycosides', located in the brush border surface membrane of small intestinal cells that take part in the last step of carbohydrate digestion. These enzymes exclusively catalyse the hydrolysis of α-1,2, α-1,4 and α -1,6-glucosidic linkages in oligosaccharides and thereby release absorbable monosaccharides (Sim et al., 2008). Currently, acarbose, miglitol and voglibose are used as alpha glucosidase inhibitors (AGI) which are isolated from microbes. Unfortunately, severe adverse effects like vomiting, liver disorders, flatulence, abdominal discomfort, hypoglycaemia, urinary tract infection, etc. have been noticed in patients medicated with acarbose, miglitol and voglibose. Even though, the acarbose is a common drug prescribing as an AGI to treat T2DM (Dabhi et al., 2013; Mitrakou et al., 1998; Van De Laar et al., 2005).

Chronic hyperglycaemia is a condition observed in all forms of DM. According to the earlier reports, hyperglycaemia activates several biochemical pathways in the cells that are prone to the accumulation of

* Corresponding author.
E-mail address: annuk9@yahoo.co.in (A. Kulal).

https://doi.org/10.1016/j.heliyon.2020.e04392
Received 23 October 2019; Received in revised form 31 January 2020; Accepted 1 July 2020

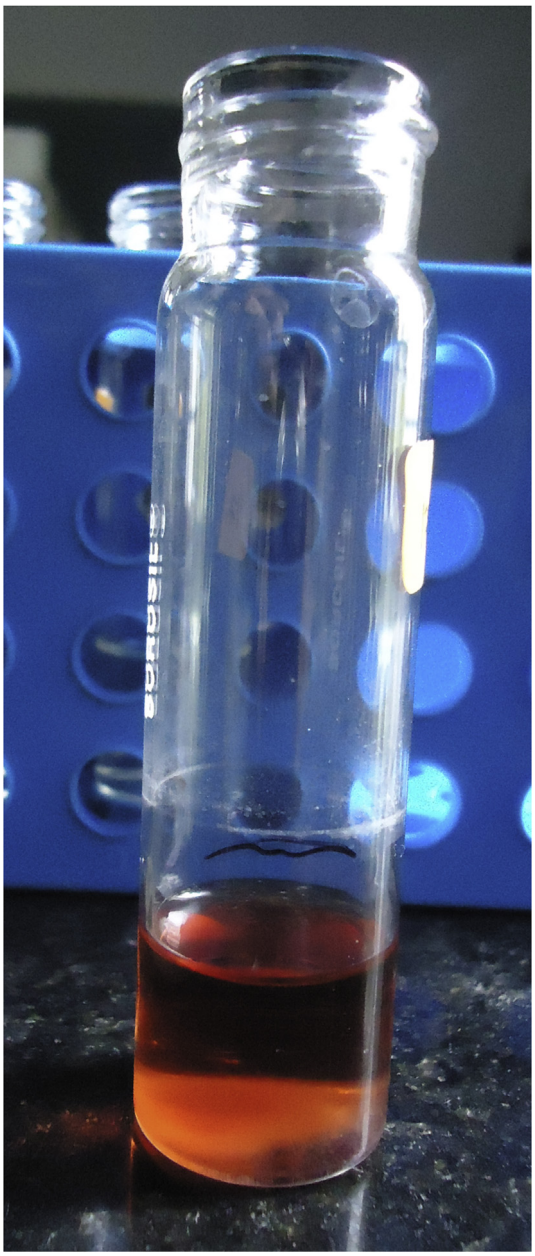

Figure 1. Silica gel column purified phenolic rich 'fraction-14'. Out of 16 fractions colleced from the silica gel column chromatography of ethanol extract from *S. glauca* leaf, the 'fraction-14' had high phenolic content and found to be highly active against alpha glucosidase enzyme.

reactive oxygen species (ROS). Because of dearth in the proper endogenous antioxidant defence mechanism, excessively accumulated ROS activates the stress-sensitive intracellular signalling pathways, which in turn, promote the cellular damage and play a role in the development of diabetic complications (Giacco and Brownlee, 2010; Vanessa Fiorentino et al., 2013). Among the several compounds that have been identified as AGI, generally phenolic compounds from a natural source are identified as the main phytochemicals with antioxidant properties. They work by reducing the accumulation of ROS in diabetic complications (Alam et al., 2017; Chen et al., 2019; Sarikurkcu et al., 2019). Also, flavonoids, phenylpropanoids, terpenes and quinines are known as good inhibitors of the alpha glucosidase enzyme as listed in a review (Yin et al., 2014). Even though myriad of phytochemical compounds have been reported from plant sources, there are no reports on the commercialization of phytochemicals as AGI so far. This lacuna was the drive for investigations to find a more potent natural AGI molecule from *Simarouba glauca* plant.

Simarouba glauca DC is rain-fed wasteland tree commonly called as 'Laxmitaru' or 'Paradise tree' belonging to the family Simaroubaceae. Different parts of the plant are being used traditionally as, antifungal, antibacterial, antioxidant (Osagie-Eweka et al., 2016; Santhosh et al., 2016; Umesh, 2015), antiparasitic, antipyretic and anticancer agents (Jose et al., 2019; Manasi and Gaikwad, 2011). The bark extract of this tree is commonly used for dysentery hence the bark is also called 'dysentery-bark' (Santhosh et al., 2016; Manasi and Gaikwad, 2011). The seed powder is being used to treat snakebites (Manasi and Gaikwad, 2011). Along with other species of Simaroubaceae family, *S. glauca* also contains a unique group of active compounds called quassinoids (ailanthinone, glaucarubinone, and holacanthone) which are shown to be responsible for the wide spectrum of biological activities of this plant (Alves et al., 2014). Hence, owing to the numerous biological activities reported in earlier studies and lack of comprehensive studies on phytochemical analysis, antioxidant and AGI activities from *S. glauca*, this plant was selected to explore the correlation between phytochemicals and different biological activities.

In this study, crude and purified 'fraction-14' from the ethanol extract of *S. glauca* leaves were analysed for phytochemicals and antioxidant assay followed by yeast alpha glucosidase enzyme inhibition assay. Further, the active 'fraction-14' was characterized by HPLC-Q–TOF-MS analysis and four compounds were tentatively identified for the first time in *S. glauca* leaf extract. The efficacy of alpha glucosidase enzyme inhibition was also studied by enzyme kinetics for purified 'fraction-14'. The binding affinities of the identified compounds were analysed by *in-silico* docking of these compounds to alpha glucosidase enzyme. This study is expected to provide new insight into the potentiality of natural alpha glucosidase enzyme inhibitors as a alternative for the existing AGI to inhibit human alpha glucosidase.

Table 1. Alpha-glucosidase inhibitory (AGI) activity, phytochemical analysis, antioxidant activity of ethanol crude extract and column purified 'fraction-14' of *S. glauca* leaf.

Sample	AGI activity (IC_{50} μg/mL)	Phytochemicals		Antioxidant activity (IC_{50} in μg/mL)	
		Total phenolics (mg GA/g)	Total flavonoids (mg Q/g)	DPPH Assay	ABTS Assay
Ethanol crude extract	0.5 ± 0.04	414 ± 11	166 ± 29	12.5 ± 0.6	4.0 ± 0.5
Purified fraction-14	2.4 ± 0.40	178 ± 70	-	14.4 ± 0.1	7.6 ± 0.5
Ascorbic acid	-	-	-	5.1 ± 0.1	3.9 ± 0.2
Acarbose	2450 ± 24	-	-	-	-

Note: AGI activity and antioxidant activity are represented by IC_{50} values. Acarbose was used as a standard for AGI activity. Total phenolics are represented in mg GA per gram of extract. Total flavonoids are represented in mg Q per gram of extract. Ascorbic acid was used as standard for antioxidant activities. All the experiments are expressed as mean ± SD (n = 3). The values are statistically significant at $p < 0.05$.
Q: Quercetin, GA: Gallic acid, SD: Standard Deviation, "-": Not determined.

2. Materials and methods

2.1. Chemicals and reagents

Alpha glucosidase from *Saccharomyces cerevisiae* (19.3 U/mg, Type1 lyophilized powder, G5003), p-Nitrophenyl-α-D-glucopyranoside (≥99%, N1377), 2, 2′-Azino-bis (3-ethylbenzothiazoline-6-sulfonic acid) diammonium salt (ABTS, ≥98%, A1888), quercetin (≥95% HPLC, Q4951), gallic acid (≥98% ACS reagent, 398225) and acarbose (PHR 1253) were procured from Sigma- Aldrich, India. 2, 2-diphenyl-1-picryl-hydrazil (DPPH, 95%, Alfa Aesar-A Johnson Matthey Company) and acetonitrile HPLC grade (4400SP, Qualigens) obtained from Thermo Fisher Scientific India Pvt. Ltd. Vitamin C Purified (≥99%, QH1Q610760) and Methanol HPLC grade (SF8SF68931, 99.7%) were purchased from Merck Specialities Private Ltd, India. Chloroform analytical grade (2H2802300, 99.8%) purchased from SD Fine Chem. Ltd. India (SDFCL). Silica gel (Mesh size: 60–120) purchased from ACME Synthetic Chemicals, India.

Table 2. Alpha-glucosidase inhibitory (AGI) activity of column purified fractions of ethanol extract from *S. glauca* leaf.

S.N.	Purified fractions	AGI activity (%Inhibition)
1	1–12	-
2	13	24.5
3	14	78.7
4	15	26.1
5	16	39.1

Note: AGI values are represented in percentage inhibition at the sample concentration of 0.05 mg/mL "-": Not observed.

2.2. Extraction and purification of active compounds

Fresh leaves were collected from *S. glauca* plants grown on the campus of Poornaprajna Institute of Scientific Research, Devanahalli, Bangalore Rural-562110, India (13.2884° N, 77.6713° E). Leaves were washed immediately in distilled water and air-dried at room temperature (RT), 28 ± 2 °C. Then, fine powder was prepared from the dried leaves using a mixer grinder and stored in polythene bags at 4 °C. The extract from the same powder was used for all the subsequent experiments.

Twenty grams of leaf powder was taken in a conical flask containing 150 mL of ethanol and the soluble content was extracted twice, using a rotary shaker at RT for 12 h. The extract in ethanol was filtered using a muslin cloth and the filtrate was centrifuged at 12,096 x g for 30 min (Eppendorf, 5810 R). The supernatant was collected and dried under vacuum using a rotary evaporator at 40 °C (IKA, RV 10 D S96). The dried extract was weighed and stored at -20 °C for further use.

The dried ethanol extract was re dissolved in absolute ethanol and was loaded on to a glass column (size of 50 × 4.5 cm) packed with the silica gel (60–120 mesh size). The column was equilibrated and eluted using a mobile phase containing chloroform, acetonitrile, and methanol at 5:4:1 ratio at a flow rate of 1 mL/min and collected 12 fractions of 10 mL each. Followed by, the same sample in the column was eluted with 50% aqueous methanol at the same flow rate and 4 fractions of 10 mL each were collected. All the 16 fractions were concentrated into 2 mL each using a rotary evaporator at 40 °C and further dried in a hot air oven at 40 °C and used for analysis.

2.3. Phytochemical assays

2.3.1. Estimation of total flavonoid

The total flavonoid content of ethanol extract and purified 'fraction-14' was determined using aluminum chloride assay (Medini et al., 2014) with slight modifications. Ethanol extract and purified 'fraction-14' were dissolved in Milli-Q water at 1 mg/ml concentration respectively,

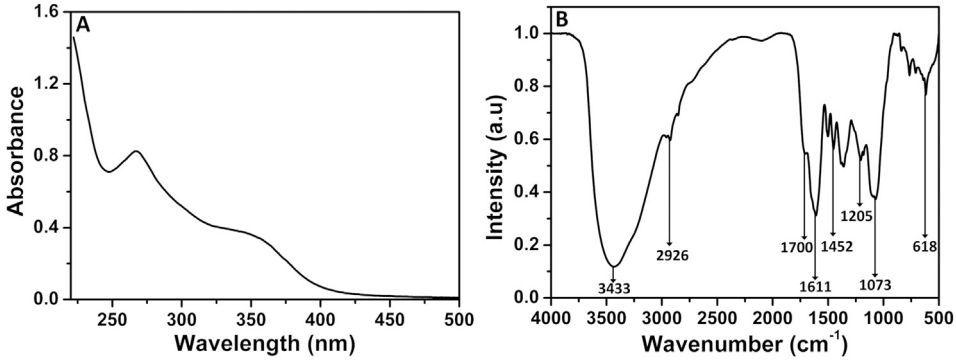

Figure 2. UV-Visible spectroscopic analysis (A) and FTIR spectra (B) of column purified 'fraction-14' of ethanol extract from *S. glauca* leaf. For UV-Visible spectroscopy, the sample was dissolved in Milli-Q water at 0.25 mg/mL concentration. For FTIR, the sample was mixed with KBr at a ratio of 1:100, ground into a fine powder and a thin pellet was made.

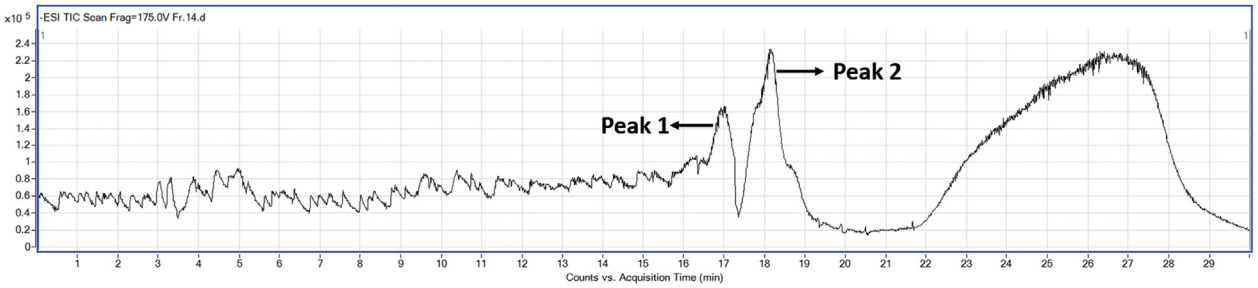

Figure 3. ESI-TIC spectra of column purified 'fraction-14'. The LC-MS peaks at retention time between 16.4-18.8 min which has high intensity was analysed for mass spectroscopy.

Table 3. LC-MS analysis of purified 'fraction-14'. The peak at retention time between 16.4-18.8 min which had high intensity was annotated for m/z values.

Show/Hide	Cpd	File	Saturated	RT	Precursor	Mass	Ion Polarity	Ions	Height	Volume	Algorithm	Quality Score
TRUE	27	Fr.14.d	-	18.139	447.0957	448.1026	Negative	8	119599	7445123	Find by Molecular Feature	100
TRUE	23	Fr.14.d	-	16.956	713.0965	714.1038	Negative	4	36790	1299330	Find by Molecular Feature	100
TRUE	26	Fr.14.d	-	17.784	599.1053	600.1123	Negative	9	36451	1476837	Find by Molecular Feature	100
TRUE	10	Fr.14.d	-	9.625	353.088	354.0953	Negative	3	27554	784165	Find by Molecular Feature	100
TRUE	30	Fr.14.d	-	18.726	417.0835	418.0908	Negative	3	23452	856989	Find by Molecular Feature	100
TRUE	22	Fr.14.d	-	16.949	577.0812	578.0884	Negative	3	20970	777064	Find by Molecular Feature	100
TRUE	2	Fr.14.d	-	3.233	362.9402	363.9474	Negative	3	20155	165424	Find by Molecular Feature	81.8
TRUE	1	Fr.14.d	-	3.039	362.9401	363.9474	Negative	3	18606	214072	Find by Molecular Feature	80
TRUE	18	Fr.14.d	-	16.215	729.0911	730.0983	Negative	4	18606	740919	Find by Molecular	100
TRUE	7	Fr.14.d	-	5.027	265.0929	266.1	Negative	5	15749	430217	Find by Molecular Feature	100
TRUE	11	Fr.14.d	-	10.571	183.03	184.0373	Negative	2	14872	541952	Find by Molecular Feature	100
TRUE	20	Fr.14.d	-	16.94	463.0883	464.0952	Negative	7	13827	571896	Find by Molecular Feature	91.3
TRUE	5	Fr.14.d	-	3.889	248.9602	249.9675	Negative	2	13548	449609	Find by Molecular Feature	100
TRUE	25	Fr.14.d	-	17.778	713.0958	714.1031	Negative	3	11945	395509	Find by Molecular Feature	100
TRUE	3	Fr.14.d	-	3.345	248.9601	249.9674	Negative	2	11416	106904	Find by Molecular Feature	100
TRUE	4	Fr.14.d	-	3.854	520.9083	521.9156	Negative	2	10581	175521	Find by Molecular Feature	100
TRUE	19	Fr.14.d	-	16.221	615.0978	616.105	Negative	6	9636	377572	Find by Molecular Feature	100
TRUE	6	Fr.14.d	-	3.928	154.9736	155.9809	Negative	2	9430	276406	Find by Molecular Feature	86.5
TRUE	16	Fr.14.d	-	12.999	633.0717	634.079	Negative	5	9163	226214	Find by Molecular Feature	100
TRUE	28	Fr.14.d	-	18.165	561.0843	562.0916	Negative	3	8935	408128	Find by Molecular	100
TRUE	9	Fr.14.d	-	6.291	169.0141	170.0214	Negative	2	8767	274588	Find by Molecular	100
TRUE	29	Fr.14.d	-	18.718	599.1034	600.1103	Negative	6	8624	495158	Find by Molecular Feature	82.1
TRUE	13	Fr.14.d	-	11.465	531.0956	532.1029	Negative	3	8351	248916	Find by Molecular Feature	100
TRUE	8	Fr.14.d	-	5.294	331.0664	332.0737	Negative	3	7720	221418	Find by Molecular Feature	100
TRUE	12	Fr.14.d	-	11.455	417.1032	418.1104	Negative	5	7289	230316	Find by Molecular Feature	87.1
TRUE	24	Fr.14.d	-	17.763	433.0768	434.0841	Negative	4	6128	231414	Find by Molecular Feature	100
TRUE	21	Fr.14.d	-	16.949	599.1024	600.109	Negative	6	5973	278252	Find by Molecular Feature	100
TRUE	17	Fr.14.d	-	15	651.1877	652.195	Negative	3	5747	180282	Find by Molecular Feature	80
TRUE	14	Fr.14.d	-	12.015	467.0797	468.0869	Negative	3	5336	198210	Find by Molecular Feature	100
TRUE	15	Fr.14.d	-	12.023	353.0873	354.0946	Negative	2	5135	154844	Find by Molecular Feature	100

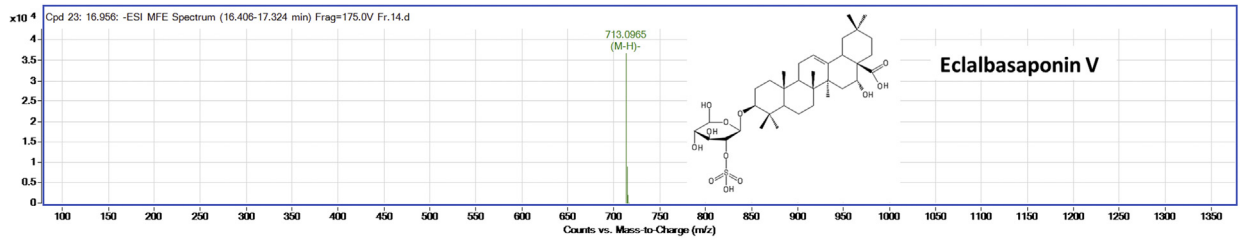

Figure 4. Mass spectra of eclalbasaponin V (compound 1). The m/z value was obtained in negative ionization mode and compared with m/z value of previously identified compounds in literature.

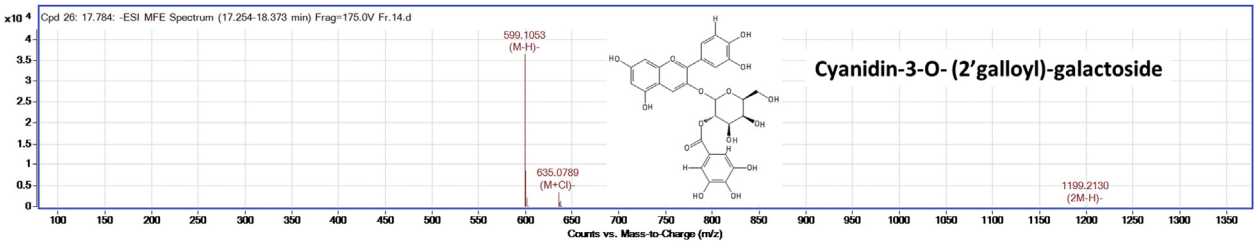

Figure 5. Mass spectra of cyanidin-3-O- (2′galloyl)-galactoside (compound 2). The m/z value was obtained in negative ionization mode and compared with m/z value of previously identified compounds in literature.

centrifuged at 16,873 x g for 10 min and filtered through 0.2 μm syringe filters before the analysis. The reaction mixture containing 150 μL of $NaNO_2$ (0.72 M) and 100 μL of the sample in a 10 mL test tube. Then, the volume was made up to 2650 μL with Milli-Q water and incubated at RT (28 °C) for 5 min. Then 150 μL of $AlCl_3$ (0.74 M) was added and incubated at RT for 1 min. Immediately after incubation, 1000 μL of NaOH (1

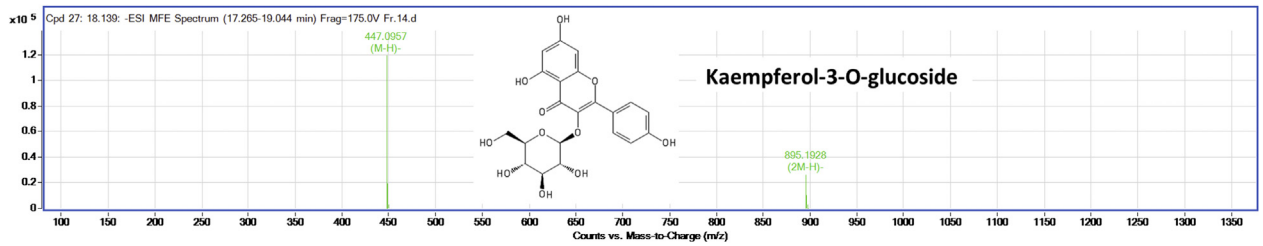

Figure 6. Mass spectra of kaempferol-3-O-glucoside (compound 3). The m/z value was obtained in negative ionization mode and compared with m/z value of previously identified compounds in literature.

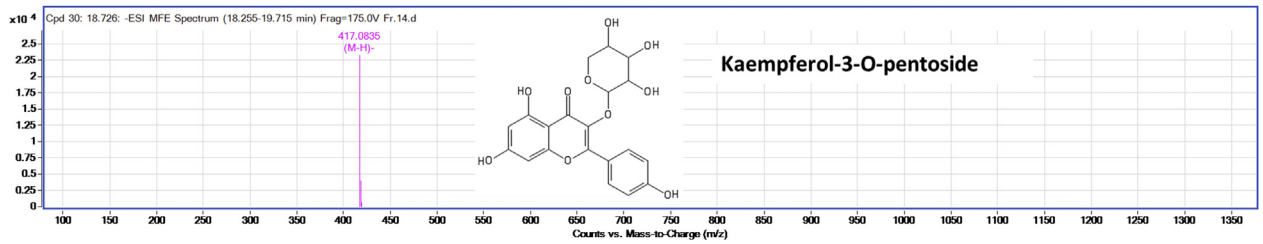

Figure 7. Mass spectra of kaempferol-3-O-pentoside (compound 4). The m/z value was obtained in negative ionization mode and compared with m/z value of previously identified compounds in literature.

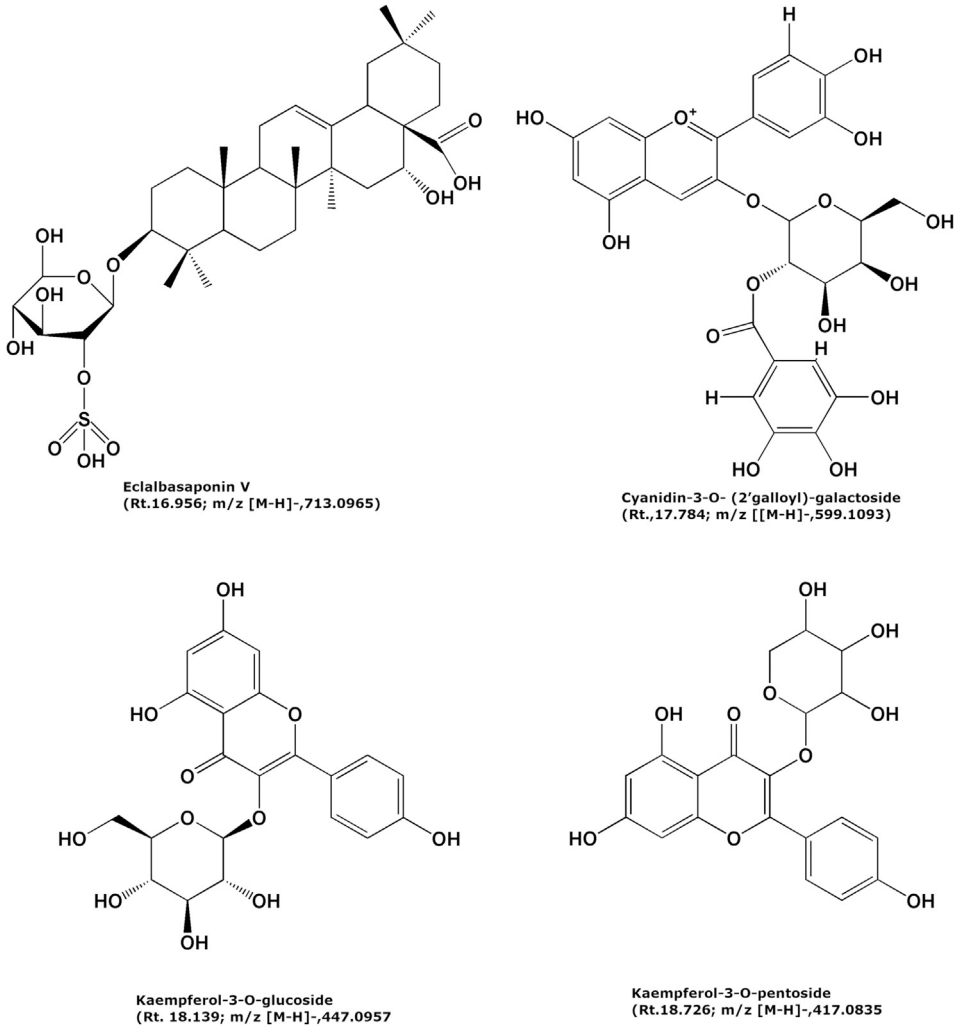

Figure 8. Chemical structures of tentatively identified compounds from column purified 'fraction-14' of ethanol extract from *S. glauca* leaf using LC-MS analysis. The compounds were identified based on the comparison of m/z values with m/z values of previously identified compounds in literature.

Table 4. Identified compounds from column purified 'fraction-14' using HPLC-Q–TOF-MS analysis.

S.N.	R_t (min)	Observed m/z [M-H]	Other fragments	m/z [M-H] from literature	Tentative identification
01	16.956	713.0965	-	713.3582	Eclalbasaponin V
02	17.784	599.1053	635.0789 [M + Cl] , 1199.2130[2M-H]	599.1039	Cyanidin-3-O- (2′galloyl)-galactoside
03	18.139	447.0957	895.1928 [2M-H]	447.0957	Kaempferol-3-O-glucoside
04	18.726	417.0835	-	417.0845	Kaempferol-3-O-pentoside

Note: The m/z values were obtained in negative ionization mode. Compounds **(S.N. 1,2, 3 & 4)**were identified based on comparison of m/z values with the previous reports. "-": Not observed.

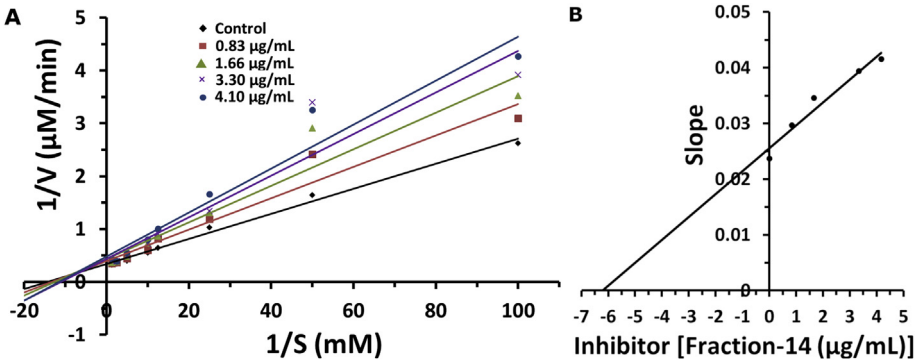

Figure 9. Lineweaver- Burk plots (A) and Secondary plot of slope versus inhibitor ('fraction-14') (B). The inhibitor concentrations were used as 0.83, 1.66, 3.32 and 4.15 µg/mL. Alpha glucosidase concentration was 0.02 units/mL. Substrate, PNPG concentrations were 0.01, 0.02, 0.04, 0.08, 0.1, 0.2, 0.4 and 0.8 mM.

Table 5. Maximum velocity; V_{max} and Michaelis-Menten constant; K_m for different concentrations of column purified 'fraction-14'.

S.N.	Fraction-14 (µg/mL)	V_{max} (µM/min.)	K_m (µM)
1	0	2.95	70
2	0.83	2.50	74
3	1.66	2.33	80
4	3.32	2.28	90
5	4.15	2.13	90

Note: The alpha glucosidase concentration was 0.02 units/mL. The substrate, PNPG concentration was 0.01, 0.02, 0.04, 0.08, 0.1, 0.2, 0.4 and 0.8 mM. The differences among the values are considered to be statistically significant at $p < 0.05$. PNPG: p-nitrophenyl-α-D-glucopyranoside.

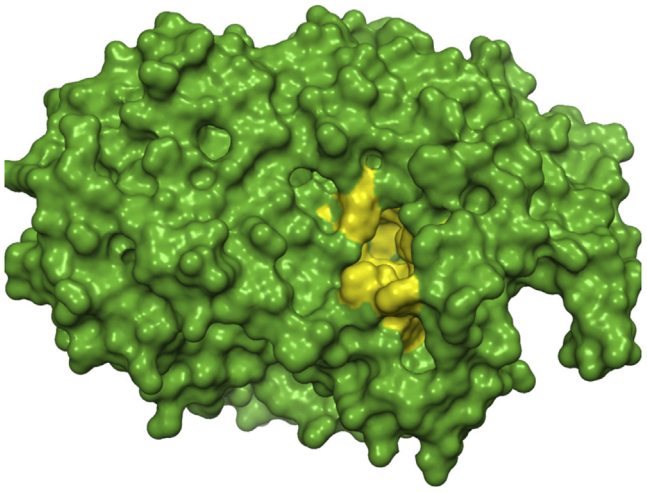

Figure 10. Surface representation of modelled structure of the yeast alpha glucosidase. The structure was generated using RaptorX software. The active site of the enzyme is represented in a yellow-colored patch where the docked compounds interacts with enzyme which involves both hydrogen bonds and hydrophobic interactions.

M) was added and the mixture was diluted to 5000 µL with Milli-Q water. The reaction mixture was mixed thoroughly and centrifuged at 16,873 x g for 5 min and absorbance was read at 510 nm using BioSpectrometer® kinetic (Eppendorf). Similarly, a standard curve was plotted for quercetin (Q) at different concentrations (200–1000 µg/mL) and used as flavonoid standard. The total flavonoid content in the sample extract was represented in milligram (mg) of quercetin equivalent/gram of the extract (mg Q/g extract).

2.3.2. Estimation of total phenolics

The total phenolic content of the ethanol extract and purified 'fraction-14' was determined using the Folin-Ciocalteu (F–C) method (Medini et al., 2014) with slight modifications. Leaf crude extract and purified 'fraction-14' were dissolved in Milli-Q water at 1 mg/ml concentration respectively, centrifuged at 16,873 x g for 10 min and filtered through 0.2 µm syringe filters before the analysis. Briefly, 200 µL of each sample was taken in a test tube and diluted to 500 µL using Milli-Q water. Then 150 µL of F–C reagent was added, stirred and kept for incubation for 6 min at room temperature. Then 1250 µL of Na_2CO_3 (1 M) was mixed thoroughly with the reaction mixture and kept for incubation in dark for 2 h. Thereafter, the reaction mixture was made up to 3 mL by diluting with 1100 µL of Milli-Q water and absorbance was measured at 760 nm using Thermoscientific Multiscan® plate reader. A standard curve was plotted using gallic acid (GA) with a concentration range of 200–1600

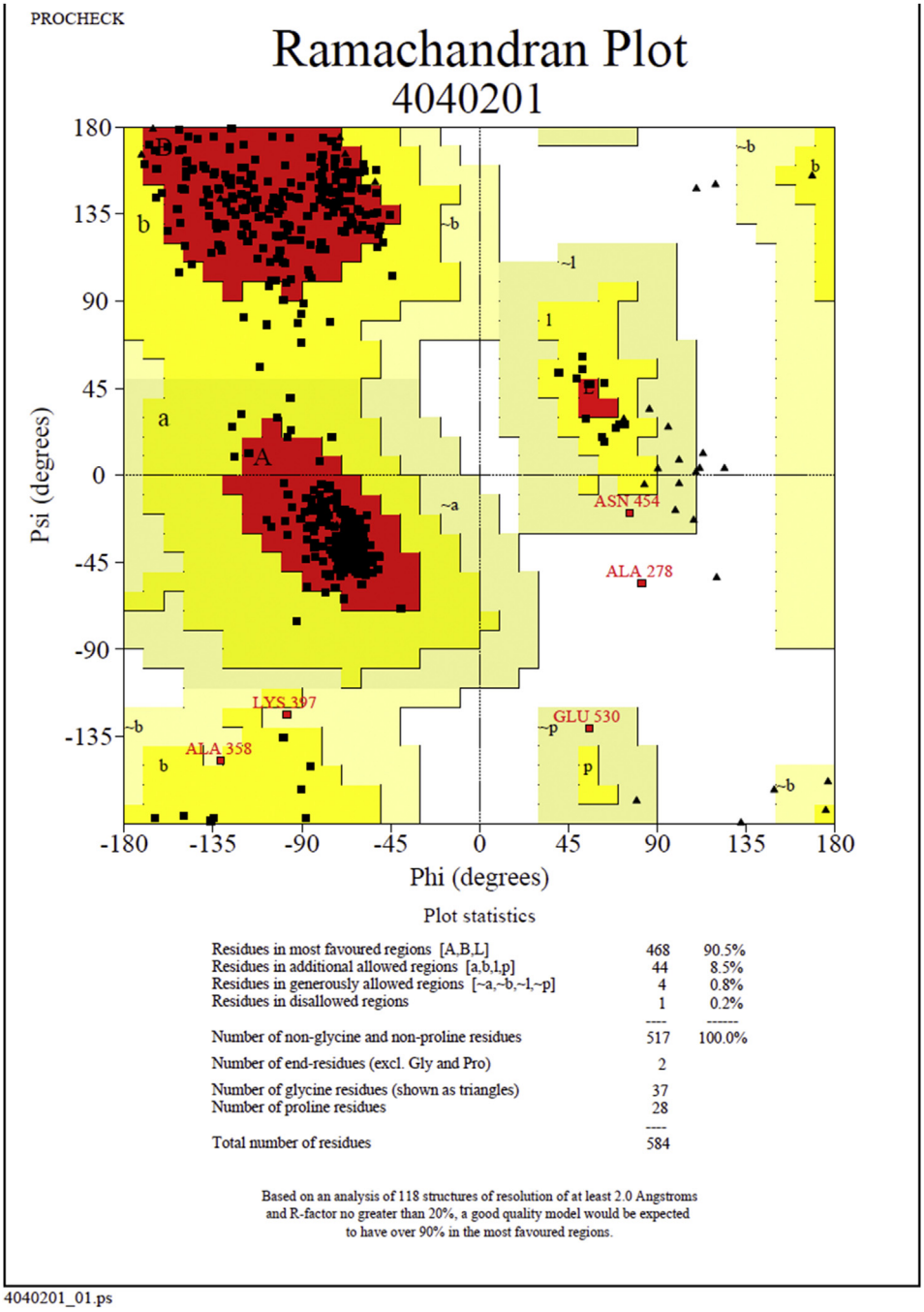

Figure 11. Ramachandran plot for homology model of yeast alpha glucosidase. The homology model was built using RaptorX software. The model was validated and authenticated by Ramachandran plot using PROCHECK software.

μg/mL. The total phenolic content was represented as mg gallic acid equivalent per gram of the extract (mg GA/g extract).

2.4. Antioxidant assays

2.4.1. DPPH assay

Ethanol crude extract and purified 'fraction-14' were dissolved in methanol at 1 mg/ml concentration, centrifuged at 16,873 x g for 10 min and filtered through 0.2 μm filter before the analysis. The DPPH free radical scavenging activity of the extract was determined using the previously described method with slight modifications (Yan et al., 2018). The reaction mixture in a 96 well plate contained 50 μl of samples at different concentrations (1, 0.5, 0.1 μg/mL; diluted in Milli-Q water) and 100 μL DPPH free radicals (0.2 mM). The final volume was made up to 200 μL with methanol and incubated at RT (28 °C) in dark for 30 min. The control was prepared by replacing the sample with the methanol. Also, sample blanks were prepared for each sample by replacing DPPH free radicals with the methanol. The absorbance was measured at 517 nm using the Thermoscientific Multiscan® plate reader. Ascorbic acid was used as a positive control at different concentration range (1.76, 3.52, 5.28, 7.04 and 8.80 μg/mL) and the standard curve was plotted. DPPH radical scavenging ability of the samples and ascorbic acid was calculated using the formula (1).

$$\text{Inhibition (\%)} = [(\text{Absorbance}_{\text{control}} - \text{Absorbance}_{\text{sample}})/\text{Absorbance}_{\text{control}}] \times 100 \quad (1)$$

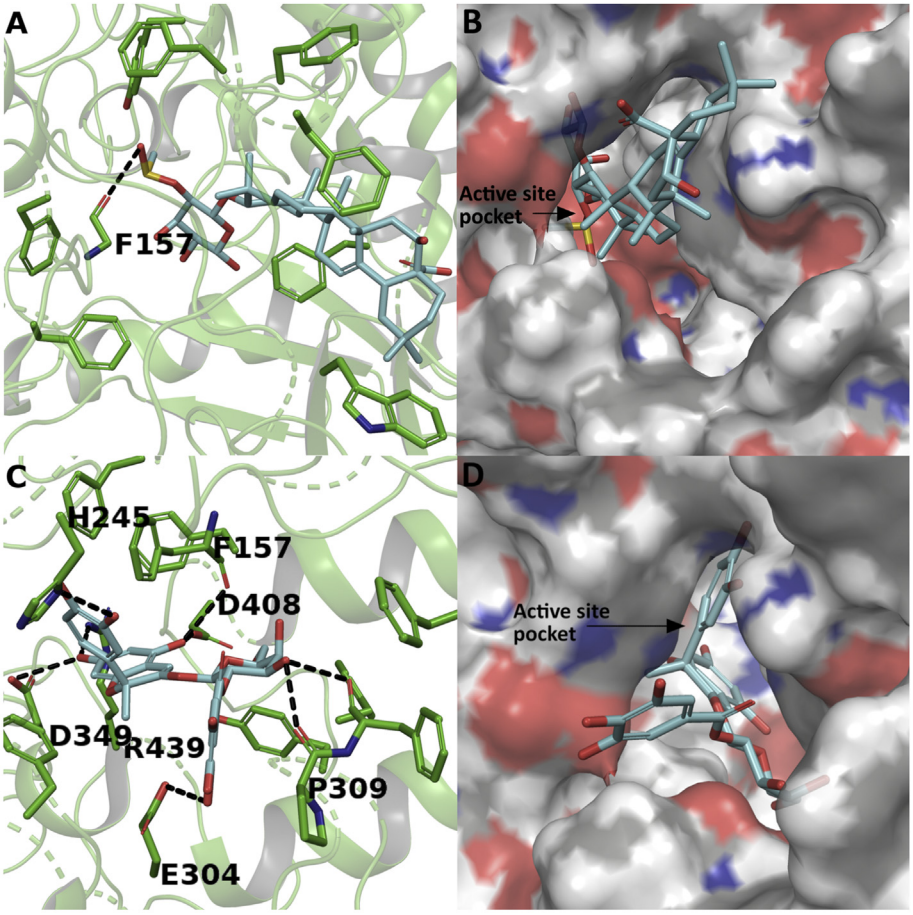

Figure 12. Docking study of compounds 1 and 2 with yeast alpha glucosidase. Interaction of compound 1 in stick representation (A) and surface representation form (B); and interaction of compound 2 in stick representation (C) and surface representation form (D) with active site residues of alpha glucosidase. The compounds were perfectly stacked inside the active site pocket of the enzyme with several hydrogen bonds and hydrophobic interactions. The hydrogen bond interactions were represented in black coloured broken lines.

The absorbance values of control and sample represented are the net values obtained after subtracting the reaction blank and sample blank respectively. The DPPH free radical scavenging activity of the samples were represented in IC_{50} values and compared with ascorbic acid (standard antioxidant).

2.4.2. ABTS assay

Ethanol crude extract and purified 'fraction-14' were dissolved in 100% methanol at 1 mg/ml concentrations, centrifuged at 16,873 x g for 10 min and filtered through 0.2 μm filter before the analysis and ABTS free radical scavenging activity was determined using the protocol previously described with slight modifications (Yan et al., 2018). The ABTS free radical was generated by incubating an equal amount of 7 mM ABTS and 2.4 mM potassium persulphate for 16 h in dark. The absorbance of the free radical was adjusted to optical density of 0.7 ± 0.03 at 734 nm by diluting in methanol. In a 96 well plate, 50 μL of the sample at different concentrations (10, 5, 1, 0.1 and 0.05 μg/mL in Milli-Q water) was taken and 100 μL of ABTS free radicals was added. The final volume was made up to 200 μL with methanol. The reaction mixture was incubated at RT (28 °C) in dark condition for 6 min. The control was prepared by replacing the sample with the methanol. Also, the sample blank was prepared for each sample by replacing ABTS free radicals with the methanol. The absorbance was measured at 734 nm using the Thermoscientific Multiscan® plate reader. Ascorbic acid was used as a positive control and the standard curve was plotted for different concentrations (0.88, 1.76, 2.64, 3.52 and 4.40 μg/mL). ABTS radical scavenging ability of the sample and ascorbic acid was calculated using the formula (2).

$$\text{Inhibition } (\%) = [(\text{Absorbance}_{\text{control}} - \text{Absorbance}_{\text{sample}})/\text{Absorbance}_{\text{control}}] \times 100 \quad (2)$$

The absorbance values of control and sample represented are the net values obtained after subtracting the reaction blank and sample blank respectively. The ABTS free radical scavenging activity of the samples were represented in IC_{50} values and compared with ascorbic acid (standard antioxidant).

2.5. Yeast alpha glucosidase inhibition (AGI) assay

Ethanol extract and purified 'fraction-14' were dissolved in Milli-Q water at 10 mg/ml concentration, centrifuged at 16,873 x g for 10 min (Eppendorf, 5418) and filtered through 0.2 μm filters before the analysis. AGI assay was carried out using the previously described method with slight modifications (Bharadwaj et al., 2018). Briefly, in a 96 well microplate, the 50 μL of sample at different concentrations (10, 5, 1, 0.1, 0.01, 0.05 and 0.005 μg/mL) mixed with 40 μL (0.0015 units/mL) of yeast alpha glucosidase enzyme and 10 μL of phosphate buffer (100 mM) pH 7. The reaction mixture was incubated at 37 °C for 20 min. Then, 50 μL of the substrate (20 mM p-nitrophenyl-α-D-glucopyranoside (PNPG) was added to the reaction mixture and incubated at 37 °C for 30 min. Immediately, 100 μL of sodium carbonate (200 mM) solution was added to the reaction mixture to retard the enzyme activity. The blank for the reaction was prepared by replacing the sample and enzyme with buffer. Similarly, the control was prepared using a buffer in place of the sample. Also, blank solutions were prepared for each sample by replacing an enzyme with a buffer. The absorbance of p-nitrophenol released during the reaction was quantified by reading at 405 nm using the Thermoscientific Multiscan® plate reader (Multiscan Go 1510). Similarly, the anti-diabetic drug acarbose was used as a standard (10 mg/mL) for the assay. The percentage of alpha glucosidase enzyme inhibition was calculated using the formula (3).

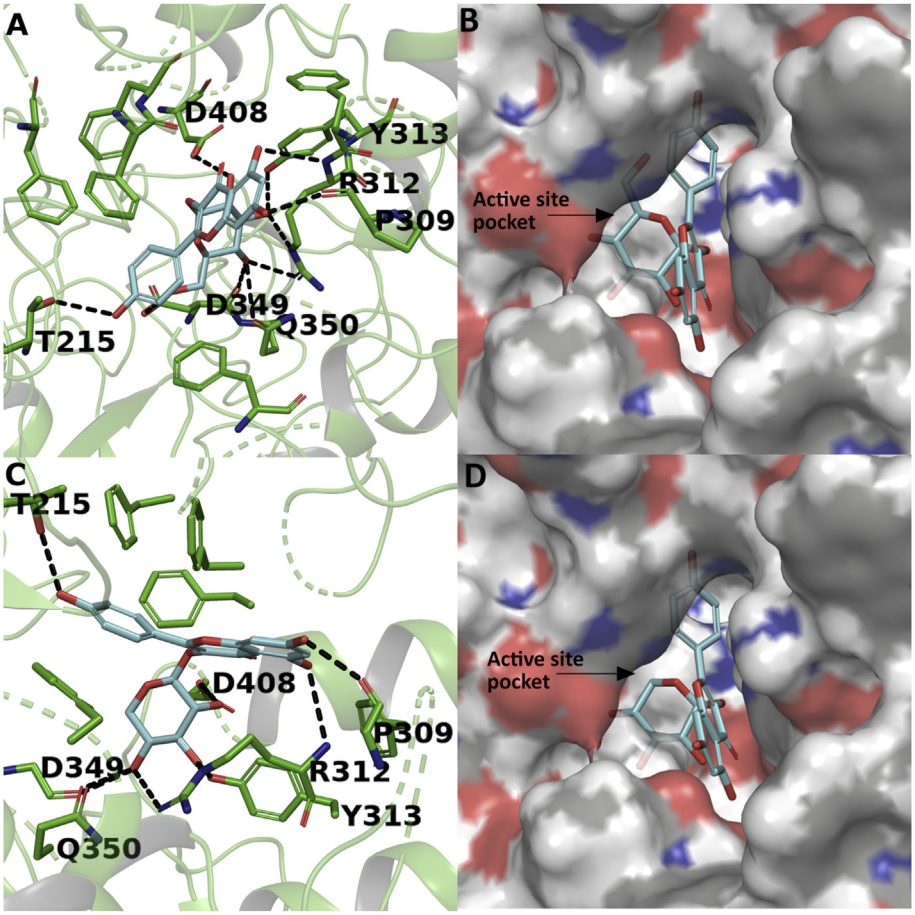

Figure 13. Docking study of compounds 3 and 4 with yeast alpha glucosidase. Interaction of compound 3 in stick representation (A) and surface representation form (B); and interaction of compound 4 in stick representation (C) and surface representation form (D) with active site residues of alpha glucosidase. The compounds were perfectly stacked inside the active site pocket of the enzyme with several hydrogen bonds and hydrophobic interactions. The hydrogen bond interactions were represented in black coloured broken lines.

Table 6. Binding energy of the compounds and interacting active site residues of *Saccharomyces cerevisiae* alpha-glucosidase.

S.N.	Compound	Binding energy (KJ/mol)	Interacting residues of the active site
1	Eclalbasaponin V	-4.409	PHE157, 310, 231, 300, 311, 158, 177, TRP242, TYR313
2	Cyanidin-3-O- (2′galloyl)-galactoside	-7.769	HIS245, PRO309, ASP408, 349, GLU304, ARG439, PHE157, 177, 310, 231, 311, 158, 300, TYR313
3	Kaempferol-3-O-glucoside	-7.127	PRO309, ARG312, THR215, ASP349, 408, TYR313, GLN350, PHE157, 158, 300, 177, 311
4	Kaempferol-3-O-pentoside	-7.04	THR215, ASP349, 408, GLN350, TYR313, ARG312, PRO309, PHE300, 157, 177, 158, 311
5	Acarbose	-6.867	PRO309, HIS239,279, ASP349, SER156, ARG439, THR215, GLU276, ASP214, PHE310, 300, 157, 177, 311, 158, TYR17, 313

Note: The hydrogen bond interactions and hydrophobic interctions were observed during the docking study.

$$\text{Inhibition } (\%) = [(\text{Absorbance}_{\text{control}} - \text{Absorbance}_{\text{sample}})/\text{Absorbance}_{\text{control}}] \times 100 \quad (3)$$

The absorbance values of control and sample represented are the net values obtained after subtracting the reaction blank and sample blank respectively. The alpha glucosidase enzyme inhibition activity of the samples was represented in IC_{50} values and compared with acarbose.

2.6. Characterization

2.6.1. UV-visible spectroscopy

The column purified 'fraction-14' was dissolved in Milli-Q water at 0.25 mg/mL concentration and UV-Visible spectra were measured. The absorbance spectrum was measured from 200-830 nm range using Bio-Spectrometer® kinetic.

2.6.2. Fourier transform infrared spectroscopy (FTIR)

The column purified 'fraction-14' was analysed using FTIR equipped with a DLATGS detector (BRUKER ALPHA). The dried sample was mixed with KBr at a ratio of 1:100 respectively and the mixture was ground into a fine powder using a mortar and pestle. The thin pellet was prepared and placed on the sample holder of the instrument and scanned at 4000 - 400 cm^{-1} range.

2.6.3. HPLC-Q–TOF-MS analysis

Column purified 'fraction-14' was further characterized using an HPLC equipped with Phenomenex C18 column (Aqua 5 μm, 200Å, 250 × 4.6 mm i.d.) to separate the analytes. Binary mobile phase system consisting solvent A: water +0.1% formic acid and solvent B: acetonitrile 90% + 0.1% formic acid with a gradient elution; 0–15 min (A:95% & B:5%), 15–17 min (A:65% & B:35%), 17–24 min (A:25% & B:75%), 24–30 min (A:95% & B 5%) was used for the elution. The separated

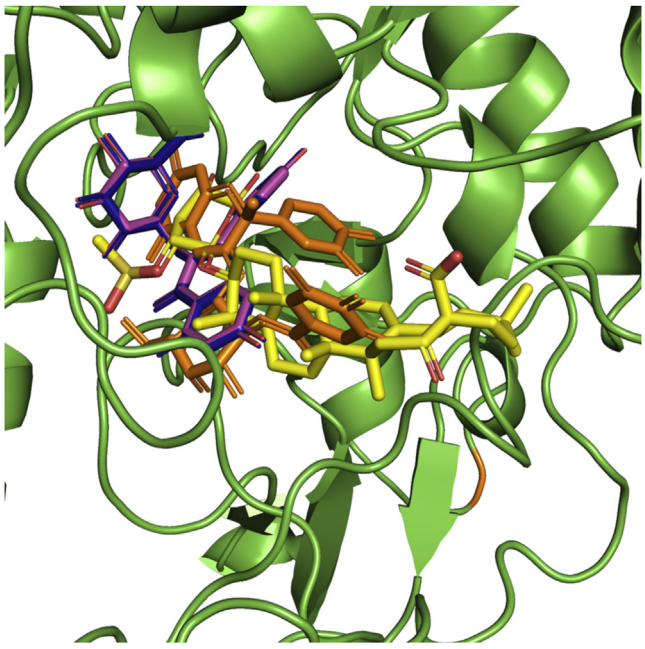

Figure 14. Superimposition of the docked compounds in the active site of the enzyme. Compounds 1, 2, 3 and 4 were represented in yellow, orange, blue and purple coloured sticks respectively.

analytes were detected from m/z 100–1000 using Accurate Mass Q-TOF-LC/MS (Agilent Technologies, 6520) equipped with dual electrospray ionization source (ESI). Analytes were identified in negative ionization mode using the following instrument conditions; gas flow, 8 L/min; gas temperature, 250 °C; nebulizer 35 psig; capillary voltage, 2750 V. The structures of identified molecules were drawn using the software ChemDraw Pro 8.0.

2.7. Enzyme inhibitory kinetics

Alpha glucosidase enzyme inhibition kinetic study was performed for column purified 'fraction-14' using a modified method previously explained elsewhere (Şöhretoğlu et al., 2018). P-nitrophenyl α-D-glucopyranoside (PNPG) was used as a substrate at different concentration range (0.01–0.8 mM). The enzyme concentration was maintained at 0.02 Units/mL for the experiment. The enzyme kinetic activity was studied in the absence as well as in the presence of inhibitors at different concentrations (0.83–4.15 μg/mL). The mode of enzyme inhibition, V_{max}, and K_m was determined using the following Lineweaver- Burk plot formula (4). The inhibitory constant K_i was determined from the graph slope versus inhibitor concentrations.

$$\frac{1}{Vo} = \left[\frac{Km}{Vmax}\right] \times \frac{1}{[S]} + \frac{1}{Vmax} \quad (4)$$

where V_0: Initial velocity; K_m: Michaelis-Menten constant; V_{max}: Maximum velocity; S: Substrate concentration.

2.8. Molecular docking

2.8.1. Homology model

The *in-vitro* studies are performed against the alpha glucosidase enzyme from *Saccharomyces cerevisiae*. The protein sequence of alpha glucosidase (MAL12-Yeast) in the FASTA format was retrieved from UniProt (access code P53341). Since the crystal structure of alpha glucosidase from *Saccharomyces cerevisiae* is not available, the 3D structure of the enzyme was generated using RaptorX homology modelling software (http://raptorx.uchicago.edu/). The quality of the homology model was authenticated by the Ramachandran plot using PROCHECK software (https://servicesn.mbi.ucla.edu/PROCHECK/).

2.8.2. Docking study

A docking study was performed against the homology model of *Saccharomyces cerevisiae* alpha glucosidase enzyme. The protein structure was prepared using the protein preparation module on Maestro with the default setting. The 2D structures of acarbose, kaempferol-3-O-pentoside and kaempferol-3-O-glucoside were retrieved from the PubChem database. Eclalbasaponin V and cyanidin-3-O- (2′galloyl)-galactoside were drawn using PubChem sketcher V2.4 software (https://pubchem.ncbi.nlm.nih.gov/edit2/index.html). The 3D conformations of compounds were generated by LigPrep (Schrodinger, LLC, New York, NY, 2015) with default settings using OPLS2005 force field. A docking grid of 20 Å was created around the enzyme active-site and the grid was identified as x: 11.33, y: -0.02 and z: 26.77. Docking was performed using Glide (Schrodinger, LLC, New York, NY, 2015) on Maestro version 10.1. The best docking poses for all the compounds were visually analysed using Pymol software (https://pymol.org/edu/?q=educational/).

2.9. Statistical analysis

The experiments were done in triplicates (n = 3) and verified as mean ± SD. The inhibition percentage and IC50 values were calculated by performing a regression analysis. Analysis of variance (ANOVA) was

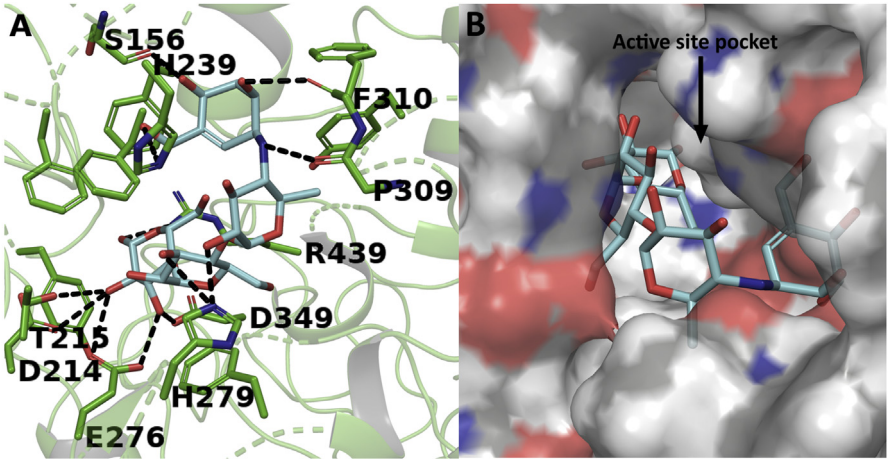

Figure 15. Docking study of acarbose with yeast alpha glucosidase. (A) Stick representation and (B) Surface representation. The hydrogen bond interactions were represented in black coloured broken lines.

implemented and the differences between the values are considered to be statistically significant at $p < 0.05$ using Microsoft Excel 2010.

3. Results and discussion

3.1. Extraction and purification of the active compounds

The 20 g dried leaf of *S. glauca* was yielded 3.6 g of ethanol crude extract, which had AGI activity. One gram of the crude extract was purified on a silica gel column and 16 fractions were collected. Each fraction was dried and analysed for the AGI activity. Out of 16 fractions, 'fraction-14' (20 mg) was found to be highly active against alpha glucosidase enzyme as represented in Figure 1. Further, the 'fraction-14' was analysed for phytochemicals and antioxidant assays along with the crude extract.

3.2. Phytochemical assays

3.2.1. Estimation of total phenolics and flavonoids

The total phenolic and flavonoid compounds of ethanol extract and purified 'fraction-14' are represented in Table 1. The total phenolic compounds in crude extract and purified 'fraction-14' were determined to be 414 ± 11 and 178 ± 7 mg GA/g of extract respectively. The total flavonoid content in crude ethanol extract was found to be 166 ± 29 mg Q/g of extract. However, flavonoid content was not detected in purified 'fraction-14' up to a concentration of 1 mg/mL. Earlier studies on *S. glauca*, Umesh et al. reported the phenolic contents of about 200 GA/g and flavonoids as 14.98 mg Q/g in the crude ethanol extract (Umesh, 2015). Another report confirmed the presence of phenolic compounds in ethanol extract as 84.55 ± 0.59 mg GA/g of extract (Puranik et al., 2017). Another group reported a very low level of phenolic and flavonoid compounds in the crude ethanol extract of *S. glauca* leaves as 0.12 ± 0.01 mg GA/g and 0.14 ± 0.02 mg Q/g of extract respectively (Osagie-Eweka et al., 2016). However, all the earlier studies are on crude ethanol extract alone.

Even though the phenolic compounds are ubiquitous in plants, their recovery greatly depends on their extraction method, solubility in the solvents, the extent of polymerization of phenols, the interference of other metabolites, the formation of insoluble complexes, etc (Medini et al., 2014). In this study, the *S. glauca* leaf extract showed a high amount of total phenolic and flavonoid compounds than the previous reports. This observation is probably due to factors such as different geographical origin of the plant, environmental conditions, seasonal differences, solvents, etc (Medini et al., 2014). Most of the earlier reports on plant extracts which had high phenolic compounds, also showed good antioxidant activity and AGI activity (Chen et al., 2019; Jiang et al., 2017; Sarikurkcu et al., 2019; Tan and Chang, 2017; Yan et al., 2018). So, the present study was focused on the antioxidant property and identification of AGI from phenolic rich purified 'fraction-14' of *S. glauca*.

3.3. Antioxidant assays

DPPH and ABTS free radical scavenging activity of ethanol extract purified 'fraction-14' and a standard were determined and expressed their IC_{50} values as shown in Table 1. The DPPH free radical scavenging activity (IC_{50}) of the ethanol extract and purified 'fraction-14' were 12.5 ± 0.6 and 14.4 ± 0.1 μg/mL respectively. Whereas, the ABTS free radical scavenging activity (IC_{50}) for ethanol extract and purified 'fraction-14' were 4 ± 0.5 and 7.6 ± 0.5 μg/mL respectively. For both the assays, ascorbic acid was used as a positive control. DPPH and ABTS free radical scavenging ability of ascorbic acid were found to be 5.1 ± 0.1 and 3.9 ± 0.2 μg/mL respectively. Both the ethanol extract and purified 'fraction-14' had lower antioxidant activity than ascorbic acid.

The antioxidant properties of the phenolic and flavonoid compounds have been studied extensively for decades. It has been reported that the antioxidant properties of the phenolics and flavonoids are due to the presence of aromatic rings containing hydroxyl groups. These hydroxyl moieties associated with an aromatic ring can donate a hydrogen atom or an electron, chelate metals, activate antioxidant enzymes or inhibit oxidases (Amarowicz et al., 2004). Crude ethanol extract from *S. glauca* leaves containing phenolic and flavonoid were shown to possess good DPPH activity (IC_{50}) of 13.12 μg/mL (Umesh, 2015) and 4.91 μg/mL (Osagie-Eweka et al., 2016). The earlier report on ABTS free radical scavenging activity for the crude ethanol extract of *S. glauca* was 45.20 μg/mL (Osagie-Eweka et al., 2016). In the present study, DPPH (IC_{50} = 12.5 ± 0.6 μg/mL) and ABTS (IC_{50} = 4 ± 0.5 μg/mL) values of crude ethanol extract (which had phenolics and flavanoids) are comparable to the antioxidant values of earlier studies. Similarly, another study on *S. glauca* leaves reported very low DPPH scavenging activity in ethyl acetate (IC_{50} = 1200 μg/mL) and petroleum ether (IC_{50} = 1280 μg/mL) extracts (Santhosh et al., 2016). However, in the present study along with alpha glucosidase inhibition, the column purified 'fraction-14' of *S. glauca* also showed the presence of phenolics, as well as DPPH and ABTS free radical scavenging activity for the first time.

3.4. Yeast alpha glucosidase inhibition (AGI) assay

The AGI activities of ethanol extract and purified 'fraction-14' were represented in Table1. The ethanol extract exhibited good activity with an IC_{50} value of 0.5 ± 0.04 μg/mL. The AGI activity of 'fraction-14' showed the highest activity than the other fractions with an IC_{50} value of 2.4 ± 0.4 μg/mL as represented in Table 1. Also, Table 2 represents the AGI activities of the remaining purified fractions of ethanol extract. Further, the crude ethanol extract and 'fraction-14' have shown very good inhibition of alpha glucosidase enzyme which are significantly better than the standard acarbose (IC_{50} = 2450 ± 24 μg/mL).

There are several reports on the AGI activity of the phenolic extracts from other plants. The phenolic extract from *Panicum sumatrense* has shown AGI activity with an IC_{50} value of 18.97 ± 0.43 μg/mL against yeast enzyme (Pradeep and Sreerama, 2018). The extractable and non-extractable polyphenols from *Camellia sinensis* exhibited yeast AGI activity with IC_{50} values of 0.77 ± 0.02 and 1.96 ± 0.21 μg/mL respectively (Yan et al., 2018). The semi-purified phenolic rich extract of *Glycine max* L showed AGI activity against yeast enzyme with an IC_{50} value of 13.81 ± 0.081 μg/mL (Tan and Chang, 2017). Also, the phenolic rich ethyl acetate extract of *Eucalyptus grandis* inhibited yeast AG enzyme with an IC_{50} value of 1.40 ± 0.18 μg/mL (Jiang et al., 2017). In another report, the phenolic extract of *Juglans regia* leaf showed AGI activity *in-vitro* and anti-hyperglycaemic effect against streptozotocin-induced rat models (Mollica et al., 2017).

However, there are few *in-vivo* studies on the anti-diabetic properties of the plant extracts from Simaroubaceae family. One study shows, the compounds bruceine E and D isolated from *Brucea javanica* lowers the blood glucose concentration by 73.57 ± 13.64% and 87.99 ± 2.91% respectively in streptozotocin-induced rat models, when compared to the non-treated streptozotocin-induced rats (NoorShahida et al., 2009). In another study, the methanolic extract of *Quassia amara at* 200 mg/kg dose reduces the elevated blood glucose level near to the normal in a streptozotocin-induced rat model (Husain et al., 2011). But there are no available reports on *the in-vitro* or *in-vivo* analysis of *S. glauca* extracts for AGI activity. Hence, based on the available reports on the biological properties of different parts of *S. glauca*, the AGI activity is reported for the first time in this study.

It was interesting to observe that the *in-vitro* analysis of the purified 'fraction-14' showed about 1000-fold better AGI activity (IC_{50} = 2.4 ± 0.4 μg/mL) when compared to the standard acarbose (IC_{50} = 2450 ± 24 μg/mL), indicating the presence of highly potent inhibitor of AG in *S. galuca* leaf extract, which may be a potential lead molecule to treat T2DM.There was a marginal decrease in AGI activity of purified 'fraction-14' when compared to the crude extract, which could be due to the synergistic effect of phenolic compounds present in the crude extract (Şöhretoğlu et al., 2018). The loss of activity in the purified fraction was

also reported in earlier studies (Tan and Chang, 2017; Yin et al., 2014). Most of the reports on different plant extracts indicate the AGI activity of the phenolic extracts. The current study also showed the correlation between high phenolics of 'fraction-14' and its AGI activity. Hence, to identify the possible compounds responsible for AGI activity, the 'fraction-14' was characterized using UV-Visible, FTIR and LC-MS techniques.

3.5. Characterization

3.5.1. UV-visible spectroscopy and FTIR analysis

The UV-visible spectroscopic analysis of the column purified 'fraction-14' showed two absorption peaks at 267 nm and 350 nm with the absorbance of 0.82 and 0.36 respectively indicating the presence of phenolic compounds as represented in Figure 2A. The above results correlate with the earlier studies, where they illustrate the presence of two absorption peaks for phenolic compounds in the range between 320 to 380 and 250–285 nm range in the UV region (Matthäus, 2002).

The FTIR analysis of purified 'fraction-14' shows several bands at different intensities as represented in Figure 2B. The band at 3433 cm^{-1} and 618 cm^{-1} may be due to stretching and bending vibration of -O-H groups respectively. The band at 2926 cm^{-1} could be attributed to the -C-H stretching of aromatics. The stretching vibration of –C=C- of aromatic rings could appear at 1611 cm^{-1}. The band appeared at 1452 cm^{-1} could be attributed to the presence of aromatic –C=C- bond. The band appeared at 1700 cm^{-1} may be due to the stretching vibration of –C=O bond. These are the common bands present in the identified compound **1** (eclalbasaponin V), **2** (cyanidin-3-O-(2′galloyl)-galactoside), **3** (kaempferol-3-O-glucoside) and **4** (kaempferol-3-O-pentoside). However, two bands appeared at 1073 and 1205cm^{-1} which may be attributed to the symmetric and asymmetric vibrations of the O=S=O group of compounds **1**. The description of FTIR bands to the respective functional groups in this study are explained in comparison with the earlier reports (González-Cabrera et al., 2018).

3.5.2. LC-MS analysis

The silica gel column purified 'fraction-14' was subjected to HPLC-Q–TOF-MS analysis to identify the possible compound responsible for the AGI activity. The LC-MS analysis of the compound showed two major peaks as represented in Figure 3. The LC-MS analysis of all the peaks of 'fraction-14' was represented in Table 3. The peaks at retention time between 16.4 - 18.8 min which had high intensity was annotated for m/z values. These m/z values were compared with the m/z values of the known phytochemical compounds, and four compounds were tentatively identified in negative ion mode. Figures 4, 5, 6, and 7 represents the Mass spectra of tentatively identified compounds. The structures of all four compounds are represented in Figure 8. The list of compounds with their m/z values along with the retention time and other data is represented in Table 4. The compound **1** with m/z 713.0965 $[M-H]^-$ is identified as eclalbasaponin V; a triterpenoid saponin has been identified previously in *Eclipta prostrata* L. The compound **2**; an anthocyanin, identified as cyanidin-3-O-(2′galloyl)-galactoside with m/z 599.1053 $[M-H]^-$ also reported previously from *Rhus coriaria* L (Abu-Reidah et al., 2015; Han et al., 2015) and *Victoria amazonica* (Han et al., 2015; Strack et al., 1992). These compounds are rarely reported in green leaves. However, there are some reports on the presence of anthocyanins in early as well as later stages of the vegetative part including leaves and petioles (Hatier and Gould, 2008; Lee, 2002). Study conducted by Manetas and group observed the presence of anthocyanins in the mature green leaves of *Rosa* sp. and *Ricinus communis* L (Manetas et al., 2002). Further, the presence of anthocyanins were documented in the leaves of tropical plants during their different stages of the development (Lee and Collins, 2001). In the present study extract was from the leaves of different age groups along with petiole, might have contained anthocyanins. The compound **3** with m/z 447.0957 $[M-H]^-$ identified as kaempferol-3-O-glucoside has been reported previously in *Pollen Typhae, Phaseolus vulgaris L* and *Flaveria bidentis* (L.) Kuntze (Chen et al., 2015; Pitura and Arntfield, 2019; Wei et al., 2011). The compound **4** identified as kaempferol-3-O-pentoside showed molecular ion peak at m/z 417.0835 $[M-H]^-$ has been identified previously in *Bauhinia* species and *Rubus grandifolius* Lowe. The compounds **3** and **4** belong to the flavonoid group (Farag et al., 2015; Gouveia-Figueira and Castilho, 2015). All the four compounds are reported in different plant species but, reported for the first time from *S. glauca.*

Although these four compounds are reported by others, there is no available literature on the biological activities of these compounds. However, biological activity was analysed for the compounds eclalbasaponin, eclalbasaponin I and eclalbasaponin II which are closely related to the compound **1** (Cho et al., 2016; Ray et al., 2013; Wang et al., 2018). Many anthocyanins, other than compound **2,** showed antioxidant activity and anti-inflammatory activities in an earlier report (Blando et al., 2018; Kong et al., 2003). Compound **3** was previously identified in *Helichrysum compactum* extract, which showed antioxidant activity (Süzgeç et al., 2005). In another study, the semi-purified fraction of legumes showed AGI activity and later on one of the compounds from this fraction was identified as kaempferol-3-O-glucoside (Tan and Chang, 2017). However, antioxidant activity, AGI activity, and antiproliferation effect have been determined in the crude extracts of *Bauhinia* species and *Euphorbia supina*, where later characterization of the extracts confirms the presence of compound **4** which is also identified in the present study as kaempferol-3-O-pentoside (Farag et al., 2015; Song et al., 2014).

Recently, many purified compounds like rhinacanthin C ($IC_{50} = 22.6 \pm 0.6$ μg/mL) (Shah et al., 2017), norathyriol ($IC_{50} = 4.22 \pm 0.19$ μg/mL) (Gu et al., 2019), mangiferin ($IC_{50} = 36.84$ μg/mL) (Sekar et al., 2019), etc. have been reported as AGI from different medicinal plants. The purified 'fraction-14' in this study showed better AGI activity ($IC_{50} = 2.4 \pm 0.4$ μg/mL) than the above-mentioned compounds. Compounds **3** and **4** identified in this study may contribute to the AGI activity and antioxidant activity observed in 'fraction-14', as these compounds are already known for alpha glucosidase inhibition and antioxidant properties according to the earlier reports (Farag et al., 2015; Song et al., 2014; Tan and Chang, 2017). So, the purified 'fraction-14' is expected to have a higher potential inhibitor for an alpha glucosidase enzyme and can be used for T2DM treatment after a detailed toxicological, *in-vivo* and clinical studies.

3.6. Enzyme inhibitory kinetics

The double reciprocal Lineweaver-Burk plot was used to determine the mode of inhibition and kinetic parameters for the column purified 'fraction-14'. Figure 9A represents the Lineweaver-Burk plot for different concentrations of inhibitor (purified 'fraction-14') analysed for different concentrations of the substrate (PNPG). In this plot all lines drawn were intersected at the second quadrant, which indicates, the purified 'fraction-14' exhibited the mixed type of inhibition on the alpha glucosidase enzyme. Also, the apparent V_{max} was slightly changed and Michaelis-Menten constant, K_m values were increasing with the increasing concentration of inhibitor as shown in Table 5. This behaviour indicate that the inhibitor prefers binding to the free enzyme rather than the enzyme-substrate complex. Precisely, Figure 9B represents the slope versus inhibitor was a linear fit, which shows, the purified 'fraction-14' has a single inhibition site or a single class of inhibition on the alpha glucosidase enzyme. Our findings are in line with previous reports where kaempferol and hesperetin show the mixed type inhibition on yeast alpha glucosidase enzyme. Interestingly, unlike acarbose (a competitive inhibitor), where its effectiveness is found to be hindered by the high concentration of carbohydrate intake, the mixed inhibitors would still be effective at lower concentration (Gong et al., 2017; Peng et al., 2016;

Rouzbehan et al., 2017). Furthermore, the inhibition constant, K_i for purified 'fraction-14' is 6.2 μg/mL which is better than the acarbose (K_i = 49 mg/mL) reported in the earlier study (Kim et al., 1999).

3.7. Homology model

The homology model of *S. cerevisiae* alpha glucosidase was generated using *S. cerevisiae* isomaltase (PDB:3A47; 71.8% sequence identity and 84.9% similarity with *S. cerevisiae* alpha glucosidase) and MalL mutant enzyme from *Bacillus subtilis* (PDB:4MB1; 41% sequence identity and 58.8% similarity with *S. cerevisiae* alpha glucosidase) as templates. Figure 10 represents the structure of *S. cerevisiae* alpha glucosidase in a surface view generated using RaptorX software. The active site of the enzyme is represented in the yellow-coloured patch where all the identified compounds are perfectly stacked during the docking study. Figure 11 represents the Ramachandran plot where 90.5% residues reside in the most favoured region, 8.5% residues reside in additional allowed regions, 0.8% residues located in generously allowed regions and 0.2% residues located in disallowed regions. Analysis of the Ramachandran plot further strengthens the quality of *the S. cerevisiae* alpha glucosidase homology model. So, the validated and analysed homology model was used for the docking study.

3.8. Docking study

A docking study was performed to predict the mode of interaction between the identified compounds and the alpha glucosidase enzyme. The homology modelling of *S. cerevisiae* alpha glucosidase and docking studies have been reported in earlier studies where several compounds were docked with the alpha glucosidase enzyme (Gollapalli et al., 2019; Picot et al., 2017; Wang et al., 2017). The docking study of the identified compounds are represented in Figure 12 and Figure 13. The binding energy of the compounds and active site residues of *S. cerevisiae* alpha glucosidase are represented in Table 6. Among the docked compounds, compound **2** showed highest binding energy as -7.769 kJ/mol followed by compound **3**, compound **4**, acarbose and compound **1** at binding energy -7.127, -7.04, -6.867 and -4.409 kJ/mol respectively. The compound **1** showed only one hydrogen bond interaction with the main-chain of residue PHE157 as shown in Figure 12A and stabilized in the active site pocket with hydrophobic interactions with residues PHE310, 231, 300, 311, 158, 177, TRP242 and TYR313 as represented in Figure 12B and Table 6. Figure 12C represents the mode of interaction between compound **2** and enzyme in a stick view. The cyanidin moiety of compound **2** showed five hydrogen bond interactions with the residues HIS245, ASP408, 349, PHE157 and ARG439. The galactoside moiety showed hydrogen bond interaction with PRO309 while GLU304 involved in the hydrogen bonding interaction with the galloyl moiety of compound **2.** Further, surface characteristic of compound **2** is perfectly complementary to the active site and stacks deep inside the active site pocket of the enzyme with several hydrophobic interactions such as PHE177, 310, 231, 311, 158, 300 and TYR313 as represented in Figure 12D and Table 6.

Similarly, the kaempferol moieties of the compounds **3** and **4** make hydrogen bond interactions with the residues THR215, PRO309, ARG312. The glucoside and pentoside moieties of both the compound are involved in hydrogenbond interaction with ARG312, ASP349, 408, TYR313 and GLN350 as represented in Figure 13A and Figure 13C. Further, both the compounds were stabilized in the active site pocket due to hydrophobic interactions with residues PHE157, 158, 300, 177, 311 as represented in Figure 13B, Figure13D and Table 6. Figure 14 represents the superimposition of the docked compounds in the active site pocket of the enzyme. Kaempferol, glucoside moieties of the compounds **3** and pentoside moiety of compound **4** were perfectly superimposed to each other, which indicates the similar kind of interactions of both the compounds with the enzyme. Also, the docking study was performed with antidiabetic drug acarbose represented in Figure 15 and Table 6. The acarvosine ring showed hydrogen bond interactions with residues PHE310, PRO309, HIS239 and SER156. The maltose unit occupied the active site pocket with hydrogen bond interaction with residues ARG439, GLU276, THR215, ASP349, HIS279 and ASP214 as represented in Figure 15A. Further, the acarbose was stabilized in the active site pocket with residues PHE310, 300, 157, 177, 311, 158, TYR71 and 313 as represented in Figure 15B and Table 6.

In this study docking of the identified compounds reported for the first time. Similar to the *in-vitro* AGI activities, identified compounds from the 'fraction-14' have shown better binding activities when compared to the standard drug acarbose. Though, there are no literature available on docking studies of these compounds, the binding energy of compounds **2, 3** and **4** with the yeast alpha glucosdiase are very promising. If the identified compounds preserve an effective binding affinity against human alpha glucosidase enzyme similar to this study, there would be an opportunity to develop these molecules into a new alpha glucosidase inhibitor.

Quassinoids and other compounds like kaempferol, amarolide, saponin, etc. have been isolated and reported in Simaroubaceae family for different biological activities including antidiabetic activity (Alves et al., 2014). But, the detailed study on antidiabetic properties of isolated compounds from Simaroubaceae family are lacking except for few studies on *Quassia amara* (Husain et al., 2011) and *Brucea javanica* plants (NoorShahida et al., 2009). In the present study, alpha glucosidase inhibition activity of the purified 'fraction-14' was analysed using *in-vitro*, *in-silico* as well as kinetic study indicates that there are effective inhibitors present in the *S. glauca* leaf extract. This study would be a inspiration for further detailed studies on these identified compounds to develop them as a novel natural alpha glucosidase inhibitor.

4. Conclusion

To the best of our knowledge, the detailed study on phytochemical analysis, antioxidant activity, AGI activity, kinetics and docking studies of purified phenolic rich fraction from *S. glauca* leaf was conducted for the first time in this report. The column purified 'fraction-14' of *S. glauca* possess high AGI activity when compared to commercial drug acarbose. The antioxidant activity and high alpha glucosidase inhibition activity of 'fraction-14' is comparable to the earlier studies and, the presence of phenolics was confirmed by phytochemical study. The strong AGI activity was proved by the inhibition kinetic study which shows the mixed type of inhibition on the alpha glucosidase enzyme. The superior K_i value than the acarbose suggests that the compounds present in the 'fraction -14' would have an effective AGI for the management of T2DM. The LC-MS analysis of purified 'fraction-14' lead to the identification of four compounds (compounds **1**, **2**, **3** and **4**), out of them, two compounds are already known for AGI activity and antioxidant activity. The docking study also showed that compounds **2**, **3** and **4** have higher binding energy than the known drug acarbose against alpha glucosidase, which indicates the identified compounds are better AGI than the acarbose. The phenolic rich and antioxidant fraction with significant AGI activity is a promising result for its application as a therapeutic agent to treat T2DM. Even though the *in-vitro* analysis exhibits excellent AGI activity, the implication of *in-vivo* studies would reveal the potentiality of these molecules before considering for the T2DM treatment.

Declarations

Author contribution statement

Kirana P Mugaranja: Conceived and designed the experiments; Performed the experiments; Analyzed and interpreted the data; Contributed reagents, materials, analysis tools or data; Wrote the paper.

Ananda Kulal: Conceived and designed the experiments; Analyzed and interpreted the data; Contributed reagents, materials, analysis tools or data; Wrote the paper.

Funding statement

This work was supported by Vision Group on Science and Technology (VGST), Govt. of Karnataka, India (CISEE/GRD No. 535/2016-17).

Competing interest statement

The authors declare no conflict of interest.

Additional information

No additional information is available for this paper.

Acknowledgements

KMP would like to thank Admar Mutt Education Foundation, Udupi, India for the fellowship and research facility.

References

Abu-Reidah, I.M., Ali-Shtayeh, M.S., Jamous, R.M., Arráez-Román, D., Segura-Carretero, A., 2015. HPLC–DAD–ESI-MS/MS screening of bioactive components from *Rhus coriaria* L.(Sumac) fruits. Food Chem. 166, 179–191.

Alam, M.A., Zaidul, I., Ghafoor, K., Sahena, F., Hakim, M., Rafii, M., Abir, H., Bostanudin, M., Perumal, V., Khatib, A., 2017. In vitro antioxidant and, α-glucosidase inhibitory activities and comprehensive metabolite profiling of methanol extract and its fractions from *Clinacanthus nutans*. BMC Compl. Alternative Med. 17 (181), 1–10.

Alves, I.A., Miranda, H.M., Soares, L.A., Randau, K.P., 2014. Simaroubaceae family: botany, chemical composition and biological activities. Revista Brasileira de Farmacognosia 24 (4), 481–501.

Amarowicz, R., Pegg, R., Rahimi-Moghaddam, P., Barl, B., Weil, J., 2004. Free-radical scavenging capacity and antioxidant activity of selected plant species from the Canadian prairies. Food Chem. 84 (4), 551–562.

Blando, F., Calabriso, N., Berland, H., Maiorano, G., Gerardi, C., Carluccio, M.A., Andersen, Ø.M., 2018. Radical scavenging and anti-inflammatory activities of representative anthocyanin groupings from pigment-rich fruits and vegetables. Int. J. Mol. Sci. 19 (169), 1–15.

Bharadwaj, S.S., Poojary, B., Nandish, S.K.M., Kengaiah, J., Kirana, M.P., Shankar, M.K., Das, A.J., Kulal, A., Sannaningaiah, D., 2018. Efficient synthesis and in silico studies of the benzimidazole hybrid scaffold with the quinolinyloxadiazole skeleton with potential α-glucosidase inhibitory, anticoagulant, and antiplatelet activities for type-II diabetes mellitus management and treating thrombotic disorders. ACS Omega 3 (10), 12562–12574.

Chatterjee, S., Khunti, K., Davies, M.J., 2017. Type 2 diabetes. Lancet 389 (10085), 2239–2251.

Chen, Y., Wang, E., Wei, Z., Zheng, Y., Yan, R., Ma, X., 2019. Phytochemical analysis, cellular antioxidant, α-glucosidase inhibitory activities of various herb plant organs. Ind. Crop. Prod. 141, 111771.

Chen, Y., Yu, H., Wu, H., Pan, Y., Wang, K., Jin, Y., Zhang, C., 2015. Characterization and quantification by LC-MS/MS of the chemical components of the heating products of the flavonoids extract in pollen typhae for transformation rule exploration. Molecules 20 (10), 18352–18366.

Cho, N.H., Shaw, J.E., Karuranga, S., Huang, Y., da Rocha Fernandes, J.D., Ohlrogge, A.W., Malanda, B., 2018. IDF Diabetes Atlas: global estimates of diabetes prevalence for 2017 and projections for 2045. Diabetes Res. Clin. Pract. 138, 271–281.

Cho, Y.J., Woo, J.-H., Lee, J.-S., Jang, D.S., Lee, K.-T., Choi, J.-H., 2016. Eclalbasaponin II induces autophagic and apoptotic cell death in human ovarian cancer cells. J. Pharmacol. Sci. 132 (1), 6–14.

Dabhi, A.S., Bhatt, N.R., Shah, M.J., 2013. Voglibose: an alpha glucosidase inhibitor. J. Clin. Diagn. Res.: J. Clin. Diagn. Res. 7 (12), 3023–3027.

Farag, M.A., Sakna, S.T., El-fiky, N.M., Shabana, M.M., Wessjohann, L.A., 2015. Phytochemical, antioxidant and antidiabetic evaluation of eight *Bauhinia* L. species from Egypt using UHPLC–PDA–qTOF-MS and chemometrics. Phytochemistry 119, 41–50.

Giacco, F., Brownlee, M., 2010. Oxidative stress and diabetic complications. Circ. Res. 107 (9), 1058–1070.

Gollapalli, M., Taha, M., Javid, M.T., Almandil, N.B., Rahim, F., Wadood, A., Mosaddik, A., Ibrahim, M., Alqahtani, M.A., Bamarouf, Y.A., 2019. Synthesis of benzothiazole derivatives as a potent α-glucosidase inhibitor. Bioorg. Chem. 85, 33–48.

Gong, Y., Qin, X.-Y., Zhai, Y.-Y., Hao, H., Lee, J., Park, Y.-D., 2017. Inhibitory effect of hesperetin on α-glucosidase: molecular dynamics simulation integrating inhibition kinetics. Int. J. Biol. Macromol. 101, 32–39.

González-Cabrera, M., Domínguez-Vidal, A., Ayora-Cañada, M., 2018. Hyperspectral FTIR imaging of olive fruit for understanding ripening processes. Postharvest Biol. Technol. 145, 74–82.

Gouveia-Figueira, S.C., Castilho, P.C., 2015. Phenolic screening by HPLC–DAD–ESI/MSn and antioxidant capacity of leaves, flowers and berries of *Rubus grandifolius* Lowe. Ind. Crop. Prod. 73, 28–40.

Gu, C., Yang, M., Zhou, Z., Khan, A., Cao, J., Cheng, G., 2019. Purification and characterization of four benzophenone derivatives from *Mangifera indica* L. leaves and their antioxidant, immunosuppressive and α-glucosidase inhibitory activities. Journal of Functional Foods 52, 709–714.

Han, L., Liu, E., Kojo, A., Zhao, J., Li, W., Zhang, Y., Wang, T., Gao, X., 2015. Qualitative and quantitative analysis of *Eclipta prostrata* L. by LC/MS. Sci. World J. 2015, 1–15.

Hatier, J.-H.B., Gould, K.S., 2008. Anthocyanin function in vegetative organs. In: Anthocyanins, Springer, pp. 1–19.

Husain, G.M., Singh, P.N., Singh, R.K., Kumar, V., 2011. Antidiabetic activity of standardized extract of *Quassia amara* in nicotinamide–streptozotocin-induced diabetic rats. Phytother Res. 25 (12), 1806–1812.

Jiang, P., Xiong, J., Wang, F., Grace, M.H., Lila, M.A., Xu, R., 2017. α-Amylase and α-glucosidase inhibitory activities of phenolic extracts from Eucalyptus grandis × E. urophylla bark. J. Chem. 2, 1–7.

Jose, A., Kannan, E., Kumar, P.R.A.V., Madhunapantula, S.V., 2019. Therapeutic potential of phytochemicals isolated from *Simarouba glauca* for inhibiting cancers: a review. Sys. Rev. Pharm. 10 (1), 73–80.

Kahn, S.E., Cooper, M.E., Del Prato, S., 2014. Pathophysiology and treatment of type 2 diabetes: perspectives on the past, present, and future. Lancet 383 (9922), 1068–1083.

Kim, M.-J., Lee, S.-B., Lee, H.-S., Lee, S.-Y., Baek, J.-S., Kim, D., Moon, T.-W., Robyt, J.F., Park, K.-H., 1999. Comparative study of the inhibition of α-glucosidase, α-amylase, and cyclomaltodextrin glucanosyltransferase by acarbose, isoacarbose, and acarviosine–glucose. Arch. Biochem. Biophys. 371 (2), 277–283.

Kong, J.-M., Chia, L.-S., Goh, N.-K., Chia, T.-F., Brouillard, R., 2003. Analysis and biological activities of anthocyanins. Phytochemistry 64 (5), 923–933.

Lee, D.W., 2002. Anthocyanins in leaves: distribution, phylogeny and development. Adv. Bot. Res. 37, 37–53.

Lee, D.W., Collins, T.M., 2001. Phylogenetic and ontogenetic influences on the distribution of anthocyanins and betacyanins in leaves of tropical plants. Int. J. Plant Sci. 162 (5), 1141–1153.

Manasi, P.S., Gaikwad, D., 2011. A critical review on medicinally important oil yielding plant laxmitaru (*Simarouba glauca* DC.). J. Pharmaceut. Sci. Res. 3 (4), 1195–1213.

Manetas, Y., Drinia, A., Petropoulou, Y., 2002. High contents of anthocyanins in young leaves are correlated with low pools of xanthophyll cycle components and low risk of photoinhibition. Photosynthetica 40 (3), 349–354.

Matthäus, B., 2002. Antioxidant activity of extracts obtained from residues of different oilseeds. J. Agric. Food Chem. 50 (12), 3444–3452.

Medini, F., Fellah, H., Ksouri, R., Abdelly, C., 2014. Total phenolic, flavonoid and tannin contents and antioxidant and antimicrobial activities of organic extracts of shoots of the plant *Limonium delicatulum*. Journal of Taibah University for science 8 (3), 216–224.

Mitrakou, A., Tountas, N., Raptis, A., Bauer, R., Schulz, H., Raptis, S., 1998. Long-term effectiveness of a new α-glucosidase inhibitor (BAY m1099-miglitol) in insulin-treated Type 2 diabetes mellitus. Diabet. Med. 15 (8), 657–660.

Mollica, A., Zengin, G., Locatelli, M., Stefanucci, A., Macedonio, G., Bellagamba, G., Onaolapo, O., Onaolapo, A., Azeez, F., Ayileka, A., 2017. An assessment of the nutraceutical potential of *Juglans regia* L. leaf powder in diabetic rats. Food Chem. Toxicol. 107, 554–564.

NoorShahida, A., Wong, T.W., Choo, C.Y., 2009. Hypoglycemic effect of quassinoids from *Brucea javanica* (L.) Merr (Simaroubaceae) seeds. J. Ethnopharmacol. 124 (3), 586–591.

Osagie-Eweka, S.D.E., Orhue, N.J., Ekhaguosa, D.O., 2016. Comparative phytochemical analyses and in-vitro antioxidant activity of aqueous and ethanol extracts of *Simarouba glauca* (paradise tree). Eur. J. Med. Plants 13 (3).

Peng, X., Zhang, G., Liao, Y., Gong, D., 2016. Inhibitory kinetics and mechanism of kaempferol on α-glucosidase. Food Chem. 190, 207–215.

Picot, M.C., Zengin, G., Mollica, A., Stefanucci, A., Carradori, S., Mahomoodally, M., 2017. In vitro and in silico studies of mangiferin from Aphloia theiformis on key enzymes linked to diabetes type 2 and associated complications. Med. Chem. 13 (7), 633–640.

Pitura, K., Arntfield, S.D., 2019. Characteristics of flavonol glycosides in bean (*Phaseolus vulgaris* L.) seed coats. Food Chem. 272, 26–32.

Pradeep, P., Sreerama, Y.N., 2018. Phenolic antioxidants of foxtail and little millet cultivars and their inhibitory effects on α-amylase and α-glucosidase activities. Food Chem. 247, 46–55.

Puranik, S.I., Ghagane, S.C., Nerli, R.B., Jalalpure, S.S., Hiremath, M.B., 2017. Evaluation of in vitro antioxidant and anticancer activity of *Simarouba glauca* leaf extracts on T-24 bladder cancer cell line. Phcog. J. 9 (6), 906–912.

Ray, A., Bharali, P., Konwar, B., 2013. Mode of antibacterial activity of eclalbasaponin isolated from Eclipta alba. Appl. Biochem. Biotechnol. 171 (8), 2003–2019.

Rouzbehan, S., Moein, S., Homaei, A., Moein, M.R., 2017. Kinetics of α-glucosidase inhibition by different fractions of three species of Labiatae extracts: a new diabetes treatment model. Pharmaceut. Biol. 55 (1), 1483–1488.

Santhosh, S.K., Venugopal, A., Radhakrishnan, M.C., 2016. Study on the phytochemical, antibacterial and antioxidant activities of *Simarouba glauca*. South Indian Journal of Biological Sciences 2 (1), 119-124.

Sarikurkcu, C., Eskici, M., Karanfil, A., Tepe, B., 2019. Phenolic profile, enzyme inhibitory and antioxidant activities of two endemic Nepeta species: *Nepeta nuda* subsp. glandulifera and *N. cadmea*. South Afr. J. Bot. 120, 298–301.

Sekar, V., Chakraborty, S., Mani, S., Sali, V., Vasanthi, H., 2019. Mangiferin from *Mangifera indica* fruits reduces post-prandial glucose level by inhibiting α-glucosidase and α-amylase activity. South Afr. J. Bot. 120, 129–134.

Shah, M.A., Khalil, R., Ul-Haq, Z., Panichayupakaranant, P., 2017. α-Glucosidase inhibitory effect of rhinacanthins-rich extract from *Rhinacanthus nasutus* leaf and

synergistic effect in combination with acarbose. Journal of Functional Foods 36, 325–331.
Sim, L., Quezada-Calvillo, R., Sterchi, E.E., Nichols, B.L., Rose, D.R., 2008. Human intestinal maltase–glucoamylase: crystal structure of the N-terminal catalytic subunit and basis of inhibition and substrate specificity. J. Mol. Biol. 375 (3), 782–792.
Şöhretoğlu, D., Sari, S., Şoral, M., Barut, B., Özel, A., Liptaj, T., 2018. Potential of Potentilla inclinata and its polyphenolic compounds in α-glucosidase inhibition: kinetics and interaction mechanism merged with docking simulations. Int. J. Biol. Macromol. 108, 81–87.
Song, Y., Jeong, S.W., Lee, W.S., Park, S., Kim, Y.-H., Kim, G.-S., Lee, S.J., Jin, J.S., Kim, C.-Y., Lee, J.E., 2014. Determination of polyphenol components of Korean prostrate spurge (Euphorbia supina) by using liquid chromatography—tandem mass spectrometry: overall contribution to antioxidant activity. Journal of analytical methods in chemistry 418690, 1–8.
Strack, D., Wray, V., Metzger, J.W., Grosse, W., 1992. Two anthocyanins acylated with gallic acid from the leaves of Victoria amazonica. Phytochemistry 31 (3), 989–991.
Süzgeç, S., Meriçli, A.H., Houghton, P.J., Çubukçu, B., 2005. Flavonoids of *Helichrysum compactum* and their antioxidant and antibacterial activity. Fitoterapia 76 (2), 269–272.
Tan, Y., Chang, S.K., 2017. Digestive enzyme inhibition activity of the phenolic substances in selected fruits, vegetables and tea as compared to black legumes. Journal of functional foods 38, 644–655.
Umesh, T., 2015. In-vitro antioxidant potential, free radical scavenging and cytotoxic activity of *Simarouba gluaca* leaves. Int. J. Pharm. Pharmaceut. Sci. 7 (2), 411–416.
Van De Laar, F.A., Lucassen, P.L., Akkermans, R.P., Van De Lisdonk, E.H., Rutten, G.E., Van Weel, C., 2005. α-Glucosidase inhibitors for patients with type 2 diabetes: results from a Cochrane systematic review and meta-analysis. Diabetes Care 28 (1), 154–163.
Vanessa Fiorentino, T., Prioletta, A., Zuo, P., Folli, F., 2013. Hyperglycemia-induced oxidative stress and its role in diabetes mellitus related cardiovascular diseases. Curr. Pharmaceut. Des. 19 (32), 5695–5703.
Wang, G., Peng, Z., Wang, J., Li, X., Li, J., 2017. Synthesis, in vitro evaluation and molecular docking studies of novel triazine-triazole derivatives as potential α-glucosidase inhibitors. Eur. J. Med. Chem. 125, 423–429.
Wang, W., Yao, G.-D., Shang, X.-Y., Gao, J.-C., Zhang, Y., Song, S.-J., 2018. Eclalbasaponin I from Aralia elata (Miq.) Seem. reduces oxidative stress-induced neural cell death by autophagy activation. Biomed. Pharmacother. 97, 152–161.
Wei, Y., Xie, Q., Fisher, D., Sutherland, I.A., 2011. Separation of patuletin-3-O-glucoside, astragalin, quercetin, kaempferol and isorhamnetin from *Flaveria bidentis* (L.) Kuntze by elution-pump-out high-performance counter-current chromatography. J. Chromatogr. A 1218 (36), 6206–6211.
Yan, S., Shao, H., Zhou, Z., Wang, Q., Zhao, L., Yang, X., 2018. Non-extractable polyphenols of green tea and their antioxidant, anti-α-glucosidase capacity, and release during in vitro digestion. Journal of Functional Foods 42, 129–136.
Yin, Z., Zhang, W., Feng, F., Zhang, Y., Kang, W., 2014. α-Glucosidase inhibitors isolated from medicinal plants. Food Science and Human Wellness 3 (3), 136–174.